On the Resolution of Dicke-Type Radiometers

FLEMMING THOMSEN, MEMBER, IEEE

Abstract—Microwave radiometers for remote sensing of the earth from a satellite are now in service. These are developed from astronomical radiometers designed for detection of interstellar radio sources. The radiometers measure the brightness temperature by comparing the received energy with an internal noise source at a well-defined radiation temperature. In the astronomical radiometers, it is traditional to use the same amount of time measuring the unknown source and the reference source. This principle has been inherited from the earth-based radiometers. As the earth brightness temperature varies very much due to the movement of the satellite, it is possible to enhance the resolution by using more time to measure the earth brightness temperature and less time measuring the stable reference source. The possible gain in resolution is limited by the gain fluctuation of the receiver.

I. Introduction

THE RADIOMETERS concerned include any radiometer switching between two white noise sources. The Dicke radiometer and the noise injection radiometer are the general best-known types. In Fig. 1, a block diagram of a general Dicke-type radiometer is shown.

The antenna signal and the reference signal include any injected noise contribution. The noise in these two branches are assumed to be white in the band considered. The post detection circuit has been branched for a separate treatment of the antenna and the reference signal. The traditional post detection circuit for symmetrical switching, where equal time is "spent" on measuring the reference and the antenna temperature is shown in Fig. 2.

The differential amplifier might consist of a diode switch followed by an LF-amplifier.

Referring to Fig. 1, it is assumed that the stability of the two integrators can be made sufficient in order to maintain the two integration times according to skewness of the switching. The differential amplifier may consist of a diode switch followed by an LF-amplifier.

A radiometer is characterized by two figures of merit.

1) The relative accuracy ΔT, which is fixed by fundamental physical phenomena such as thermal noise in the front-end of the receiver. Hence, ΔT is an expression of the accuracy, with which the antenna temperature may be measured. Due to its dependence on thermal noise, ΔT depends on the RF-bandwidth and the video bandwidth (i.e., the integration time).

Manuscript received November 1, 1982; revised May 9, 1983.

The author is with the Radar Section of the Electronic Division of the Air Materiel Command, the Royal Danish Airforce.

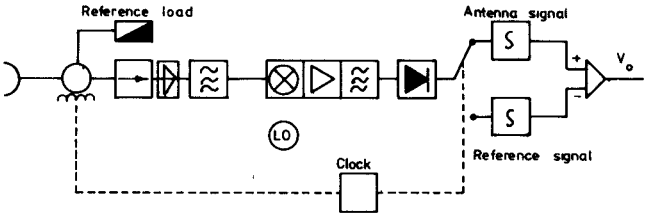

Fig. 1. Block diagram of general Dicke-type radiometer.

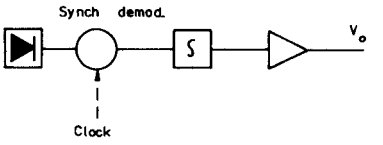

Fig. 2. Post detection section of a symmetrically switched Dicke-type radiometer.

2) The absolute accuracy, which is determined by the accuracy of the calibration, the temperature distribution of primarily the RF-components, and the RF-amplifier gain variations. The absolute accuracy indicates any offset from the correct average noise temperature. This offset generally varies with time and environmental conditions.

This paper will deal only with the relative accuracies of the general Dicke-type radiometers. An investigation of the absolute accuracy has been carried out in [1, ch. 8].

II. Calculation of the Sensitivity ΔT

When measuring the antenna noise, the input to the detector is

$$v_A(t) = q_A(t) + q_n(t) \tag{1}$$

where $q_A(t)$ is the amplified noise from the antenna referred to as the Dicke-switch, including any injected noise, and $q_n(t)$ is the noise contribution from the receiver itself.

The power spectra of the two noise signals are

$$S_A(f) = \frac{1}{2} kT_A G(f) \tag{2}$$

and

$$S_n(f) = \frac{1}{2} kT_n G(f) \tag{3}$$

where T_A and T_n are the noise temperatures of the antenna and the receiver referred to radiometer input, $G(f)$ is the

0018-9480/84/0200-0145$01.00 ©1984 IEEE

power amplification of the receiver, and k is Boltzmann's constant ($1.384 \cdot 10^{-23}$ J/K).

When switching to the reference load, the diode input voltage is

$$v_R(t) = q_R(t) + q_n(t) \tag{4}$$

where $q_R(t)$ is the noise signal caused by the reference load at temperature T_R.

The power spectrum of $q_R(t)$ is given by

$$S_R(t) = \frac{1}{2} kT_R G(f). \tag{5}$$

The duty cycle d indicates the fraction of time the switch is open to the antenna terminal. It appears a reasonable thought that more time should be spent on the unknown antenna signal than on the better known reference temperature. Applying the weights $1/d$ and $1/(1-d)$ to the reference signal and the antenna signal, respectively, the detector output V_0 turns out to be proportional to $(T_A - T_R)$. This output signal fluctuates with a standard deviation of σ_V, hence the sensitivity ΔT of the radiometer may be expressed as

$$\Delta T = \frac{\sigma_V}{\frac{\partial V_0}{\partial T}}. \tag{6}$$

As shown in Appendix A, this sensitivity can be expressed according to

$$\begin{aligned}\Delta T = \Bigg\{ & \frac{1}{B\tau_A}\left[(T_A+T_n)^2\frac{1}{d} + \frac{1}{1-d}\frac{\tau_A}{\tau_R}(T_R+T_n)^2\right] \\ & + 2\Bigg[(T_A+T_n)^2 \int_{1/2\tau_R}^{1/2\tau_A} S_g(f)\,df \\ & + (T_A-T_R)^2 \int_0^{1/2\tau_R} S_g(f)\,df\Bigg] \\ & + \Bigg[\sum_{n\neq 0} d^2 \operatorname{sinc}^2(n\pi d) \\ & \cdot \Bigg(\left(\frac{T_A+T_n}{d} + \frac{T_R+T_n}{1-d}\right)^2 \frac{1}{\tau_R} \\ & + \left(\frac{T_A+T_n}{d}\right)^2 \left(\frac{1}{\tau_A} - \frac{1}{\tau_R}\right)\Bigg) \bar{S}_g(nf_m)\Bigg]\Bigg\}^{1/2}\end{aligned} \tag{7}$$

where

$$B = \frac{\left(\int_{-\infty}^{\infty} G(f)\,df\right)^2}{2\int_{-\infty}^{\infty} G^2(f)\,df} \qquad (= \text{Bandwidth})$$

and where τ_A is the integration time for the antenna signal (limited by the available measurement time), τ_R is the integration time for the reference load signal, f_m is the Dicke frequency, $S_g(f)$ is the power spectrum of receiver gain fluctuations, $\bar{S}_g(f_m)$ is the average of S_g around the frequency f_m, and

$$\operatorname{sinc}(x) = \sin x/x$$

$$\sum_{n\neq 0} d^2 \operatorname{sinc}^2(n\pi d) = d(1-d).$$

From (7) it appears that there are three contributions to ΔT. The first is the fundamental "radiometer equation," not taking into account any gain fluctuations of the receiver. This is corrected for by the second term. The third term accounts for the noise contributions due to the harmonics of the switch frequency f_m.

The first term may be interpreted as the variance of the difference signal from two ideal total power radiometers measuring the antenna noise and the reference load, respectively.

Although the correlation between the antenna signal $v_A(t)$ and the reference signal $v_R(t)$ ($v_A(t)$ and $v_R(t)$ are correlated through the low-frequency component of the system noise $q_n(t)$) does not appear to have any influence on ΔT, the detailed derivation in Appendix A shows that this correlation actually reduces ΔT. However, this reduction vanishes due to contribution of noise from frequencies around the harmonics of the Dicke frequency; this is sketched in Fig. 3. Neglecting the correlation between the two branches thus results in a higher value of ΔT than is actually correct (see [8]).

From (7) it also appears that low-frequency gain fluctuations have a severe influence on the radiometer sensitivity.

Measurement of amplifier gain fluctuations are generally not available due to the difficulty of such measurements. Yerbury [13], however, has presented the power spectrum of the total RF-section and described the spectrum by the relation

$$S_g(f) = S_{g0}\left(\frac{f_0}{f}\right)^{\beta}, \qquad 0 < \beta < 2 \tag{8}$$

where S_{g0} is the noise power density at the "noise corner" f_0. This relation expresses the normal $1/f$-noise phenomena. Although the video bandwidth in radiometers is always limited at the lower end in order to eliminate local oscillator noise, the amplifier gain fluctuations remain a problem of concern.

A. Sensitivity of the Dicke Radiometer

For the normal Dicke radiometer, (7) reduces to

$$\Delta T \cong \left\{\frac{4}{B\tau}\frac{1}{2}\left((T_A+T_n)^2 + (T_R+T_n)^2\right) + (T_A-T_R)^2\left(\frac{\Delta G}{G}\right)^2\right\}^{1/2} \tag{9}$$

using

$$\tau_A = \tau_R = \tau \qquad \text{for } d = \frac{1}{2}$$

$$S_g(nf_g) \ll S_g(0)$$

$$\left(\frac{\Delta G}{G}\right)^2 = \int_{-1/2\tau}^{1/2\tau} S_g(f)\,df. \tag{10}$$

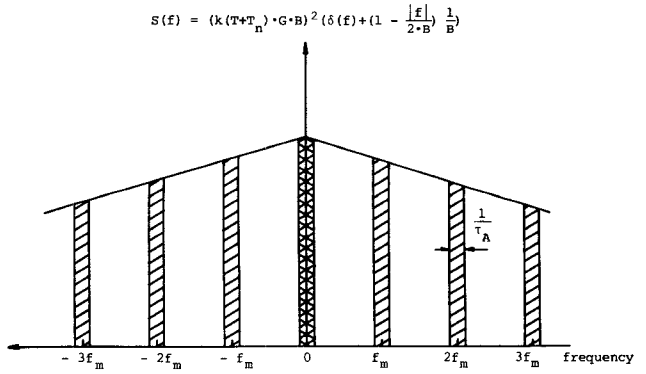

Fig. 3. Parts of post detection spectrum contributing to the noise signal at the detector output. ▦ Ideal total power received. ▨ Square modulated Dicke-type radiometer.

Equation (9) is the usual expression for the sensitivity of the Dicke radiometer, as found by several authors.

B. Sensitivity of the Noise Injection Radiometer

In the noise injection radiometer, noise from a local noise source is added to the antenna noise so as to make $T_A = T_R$ (the two temperatures measured in the two switch positions). In case of symmetrical switching, $d = 1/2$ and $\tau_A = \tau_R = \tau$, the sensitivity is found to be

$$\Delta T = 2(T_R + T_n)\left\{\frac{1}{B\tau} + \frac{1}{\tau}\sum_{n=-\infty}^{\infty} \operatorname{sinc}^2\left((2n+1)\frac{\pi}{2}\right) \cdot \bar{S}_g((2n+1)f_m)\right\}^{1/2}. \quad (11)$$

Due to the fact that $\bar{S}_g((2n+1)f_s) \ll S_g(0)$, this sensitivity is generally superior to the sensitivity of the Dicke radiometer. Equation (11) does agree with [9] but disagrees with the sensitivity derived, e.g., in [8].

For the case of asymmetrical switching, the sensitivity is modified to

$$\Delta T = (T_R + T_n)\left\{\frac{1}{B\tau}\left(\frac{1}{d} + \frac{\alpha}{1-d}\right) + 2\int_{\alpha/2\tau_A}^{1/2\tau_A} S_g(f)\,df + \frac{1}{\tau_A}\sum_{n\neq 0} d^2 \operatorname{sinc}^2(\pi n d) \cdot \left(\left(\frac{1}{d} + \frac{1}{1-d}\right)^2 \alpha + \frac{1}{d}(1-\alpha)\right)\bar{S}_g(nf_m)\right\}^{1/2} \quad (12)$$

where

$$\alpha = \frac{\tau_A}{\tau_R}$$

and $\bar{S}_g(nf_m)$ is the average gain fluctuation around nf_m.

From (11) it appears that increasing the duty cycle d ($d > 0.5$), hence decreasing α, reduces the first and the third term and increases the second term. The optimum choice of d and α depends on the actual gain fluctuation power spectrum at low frequencies (see Fig. 4).

Comparing (11) and (12) reveals that the sensitivity may be improved by a factor of up to two by proper choice of the switching sequence. However, this improvement seriously depends on the low-frequency gain fluctuations.

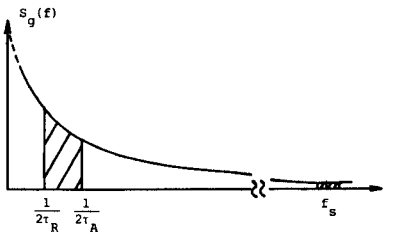

Fig. 4. Noise contributed by the gain fluctuation power spectrum.

III. Application of the Theory

An airborne multifrequency radiometer system has been developed at the Electromagnetics Institute, Technical University of Denmark, by N. Skou [14]. This has been flown with success over Greenland and the surrounding oceans. The sensitivities of these radiometers have been measured (see Table I). On this basis, an estimate of $\bar{S}_g$, according to (11), has been calculated. It is to be noted that $\bar{S}_g$ is assumed constant over the few harmonics of f_m, which give a significant contribution.

The measurements give no information about the gain fluctuation in the low-frequency region ($1/\tau \simeq 10$ Hz). If (8) is applied over the frequency range from 0 Hz to f_m (order of magnitude 1 kHz) using values of $\bar{S}_g$ given in Fig. 5, the resulting noise contribution from gain fluctuations in the frequency range $0 - 1/\tau_A$ turns out so large that no advantages are gained by asymmetrical switching. However, the above assumption might be too pessimistic, and a better estimate for the gain fluctuation below $1/\tau_A$ is assumed to be

$$S_g\left(\frac{1}{\tau_A}\right) = k \cdot \bar{S}_g. \quad (13)$$

The factor k is assumed to fall in the interval $0 < k < 20$.

If $\bar{S}_g(nf_m)$ as a first approximation are assumed constant, the optimum choice of α and d may be found to be

$$d = \frac{1}{1+\sqrt{\alpha}}$$

where α ($0 < \alpha \leqslant 1$) is a solution to

$$\left(\frac{1}{\sqrt{\alpha}} + 1\right) + \left(2 + \frac{1}{\sqrt{\alpha}}\right) B\bar{S}_g - S_g\left(\frac{1}{\tau_A}\right)\alpha^{-\beta} = 0. \quad (14)$$

The improvement in the sensitivity ΔT, when applying asymmetrical switching as compared to symmetrical switching, is in the following described by the number f, defined as the ratio between the radiometer constant corresponding to asymmetrical and symmetrical switching, respectively; hence $1/2 \leqslant f \leqslant 1$.

In order to appreciate the mutual influence of the parameters introduced above, curves are drawn (Figs. 5–8) showing the optimum duty cycle, the radiometer constant c, and the ratio f as functions of the factor k ($= S_g(1/\tau_A)/\bar{S}_g$, in (13)) for various values of $\bar{S}_g$ and β (the falloff of the power spectrum, in (8)). From these curves the following may be concluded:

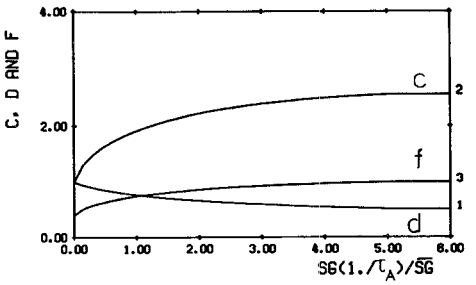

Fig. 5. Optimum duty cycle d, radiometer constant c, and the ratio f, between the radiometer constant when switching asymmetrically and symmetrically, respectively, as function of k $(=S_g(1/\tau_A)/\bar{S}_g)$. $\bar{S}_g = 5\cdot10^{-9}$ s, $\beta = 1$, and $B = 250$ MHz.

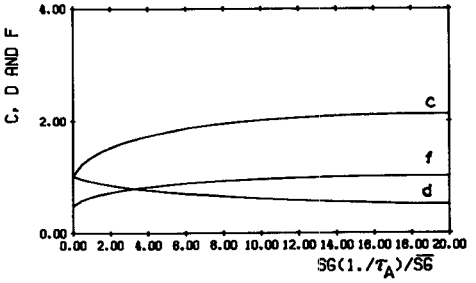

Fig. 6. Optimum duty cycle d, radiometer constant c, and the ratio f, between the radiometer constant when switching asymmetrically and symmetrically, respectively, as function of k $(=S_g(1/\tau_A)/\bar{S}_g)$. $\bar{S}_g = 10^{-9}$ s, $\beta = 1$, and $B = 250$ MHz.

TABLE I
ESTIMATE OF AMPLIFIER GAIN FLUCTUATIONS (BASED ON MEASUREMENTS OF SENSITIVITY ON TUD RADIOMETERS)

Frequency GHz	Bandwidth (2.B)	Integration Time	Refer. temp. T_R	T_n	$\sigma = \frac{2(T_R+T_n)}{\sqrt{B\tau}}$	Measured σ	$\bar{S}_g$ sec.
5	500 MHz	64 msec	13°K	100 5°K	0.67°K	0.79°K	$1.6\ 10^{-9}$
17	1 GHz	64 msec	313°K	640°K	0.34°K	0.56°K	$3.5\ 10^{-9}$
34	1 GHz	64 msec	313°K	640°K	0.34°K	0.54°K	$3.1\ 10^{-9}$

1) If the low-frequency gain fluctuations are negligible ($k_1 \simeq 0$), a factor of two is gained in the radiometer constant ($f = 1/2$) when asymmetrical switching is applied.
2) Increasing low-frequency gain fluctuations (k increasing) requires the optimum duty cycle to decrease from 1 to 1/2, resulting in an increase of the "improvement factor" f, from 1/2 to 1, corresponding to the radiometer constant for a symmetrically switched radiometer.
3) The improvement achieved by asymmetrical switching is the more pronounced, when β and $\bar{S}_g$ are small.

It should be emphasised, therefore, that low-frequency gain fluctuations have the most deteriorating effect on the radiometer performance.

IV. CONCLUSION

Future Dicke-type radiometers can be improved by introducing an asymmetrical switching technique, where more time is "spent" on measuring the varying antenna signal, and less time is used on measuring the stable reference signal. The sensitivities can be improved depending on gain fluctuations by a factor of up to two. The low frequency part of the gain fluctuation spectrum is crucial and unfortunately difficult to measure directly, because of its slight magnitude. It can, however, be determined by an asymmetrical test setup, where the sensitivity is measured as a function of the skewness of the switching. On the basis of these results, the optimum skewness of the switching can be determined.

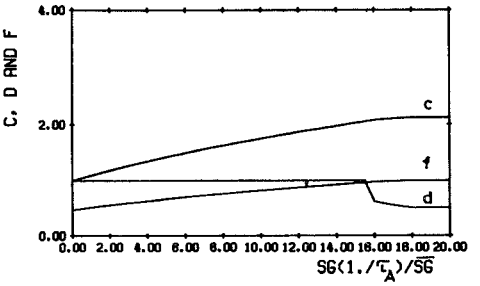

Fig. 7. Optimum duty cycle d, radiometer constant c, and the ratio f, between the radiometer constant when switching asymmetrically and symmetrically, respectively, as function of k $(=S_g(1/\tau_A)/\bar{S}_g)$. $\bar{S}_g = 10^{-9}$ s, $\beta = 0.4$, and $B = 250$ MHz.

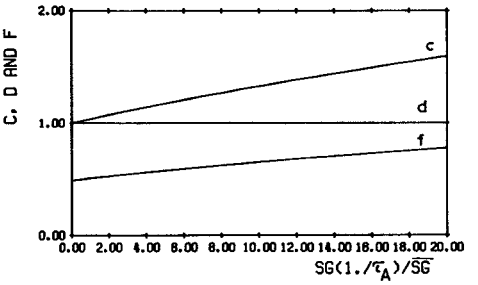

Fig. 8. Optimum duty cycle d, radiometer constant c, and the ratio f, between the radiometer constant when switching asymmetrically and symmetrically, respectively, as function of k $(=S_g(1/\tau_A)/\bar{S}_g)$. $\bar{S}_g = 5\cdot10^{-10}$ s, $\beta = 0.2$, and $B = 250$ MHz.

APPENDIX A
CALCULATION OF SENSITIVITY OF A DICKE-TYPE RADIOMETER

The square-law detector shown in Fig. 1 is assumed to have the characteristic

$$v_D = q^2. \tag{A1}$$

The input to the integrator can then be described by

$$v_0 = v_A/d - v_R/(1-d) \tag{A2}$$

d being the duty cycle of the switch function $p(t)$ as given by

$$p(t) = \begin{cases} 1, & 0 \leq |t| \leq \dfrac{d}{2f_m} \\ 0, & \dfrac{d}{2f_m} \leq |t| \leq \dfrac{1}{2f_m} \end{cases}$$

$$= d + 2d \sum_{n=1}^{\infty} \frac{\sin n\pi d}{n\pi d} \cos(n\omega_m t) \tag{A3}$$

$$p(t) = \tilde{p}(t) + d, \qquad \text{where } \langle \tilde{p} \rangle = 0 \tag{A4}$$

$$f_m = \frac{1}{2\pi}\omega_m = \text{modulation frequency.}$$

The signals v_A and v_R can be described by

$$v_A = (q_A + q_n)^2(1+g)p \tag{A5}$$

$$v_R = (q_R + q_n)^2(1+g)(1-p) \tag{A6}$$

g being a function describing the relative gain fluctuations as described by the power spectrum $S_g(f)$. The root mean square ΔG of the gain variations is given by

$$\left(\frac{\Delta G}{G}\right)^2 = \int_{-\infty}^{\infty} S_g(f)\,df. \tag{A7}$$

Using (A3), the autocorrelation function $\phi_{\tilde{p}}$ of $\tilde{p}$ can be found to be

$$\phi_{\tilde{p}}(\tau) = 2d^2 \sum_{n=1}^{\infty} \left(\frac{\sin n\pi d}{n\pi d}\right)^2 \cos(n\omega_n \tau) \tag{A8}$$

and the power spectrum

$$S_{\tilde{p}}(f) = d^2 \sum_{\substack{n\neq 0 \\ -\infty}}^{\infty} \operatorname{sinc}^2(n\pi d)\cdot\delta(f - nf_m)$$

$$\operatorname{sinc} x = \frac{\sin x}{x}. \tag{A9}$$

The mean of the output signal from the detector is given by

$$\langle v_0\rangle = \langle (q_A + q_n)^2\rangle - \langle (q_R + q_n)^2\rangle = \langle q_A^2\rangle - \langle q_R^2\rangle$$
$$= \frac{1}{2}k(T_A - T_R)\cdot\int_{-\infty}^{\infty} G(f)\,df. \tag{A10}$$

Here, it has been assumed that the noise signals q_A, q_R, and q_n are statistically independent. These signals are furthermore statistically independent of the function p and g. By the methods indicated in [10, ch. 5], the autocorrelation function of v_A is found to be

$$\phi_{v_A}(\tau) = \langle (q_A(t)+q_n(t))^2 (q_A(t+\tau)+q_n(t+\tau))^2\rangle$$
$$\cdot\langle 1 + g(t)\cdot g(t+\tau)\rangle\langle d^2 + \tilde{p}(t)\cdot\tilde{p}(t+\tau)\rangle$$
$$= \left((\mu_A+\mu_n)^2 + 2(\phi_A(\tau)+\phi_n(\tau))^2\right)$$
$$\cdot\left(1+\phi_g(\tau)\right)\left(d^2+\phi_{\tilde{p}}(\tau)\right) \tag{A11}$$

$$\mu_A = \langle q_A^2\rangle = \frac{1}{2}kT_A\int G(f)\,df \tag{A12}$$

$$\mu_n = \langle q_n^2\rangle = \frac{1}{2}kT_n\int G(f)\,df \tag{A13}$$

where ϕ_A is the autocorrelation function of the antenna signal, and ϕ_n is the autocorrelation function of the RF noise signal.

Similarly, the autocorrelation function of the reference signal at the detector output is found to be

$$\phi_{vR}(\tau) = \left((\mu_R+\mu_n)^2 + 2(\phi_R(\tau)+\phi_n(\tau))^2\right)$$
$$\cdot\left(1+\phi_g(\tau)\right)\left((1-d)^2+\phi_{\tilde{p}}(\tau)\right). \tag{A14}$$

The signals v_A and v_R are correlated because of the common noise signal q_n. The correlation function is given by

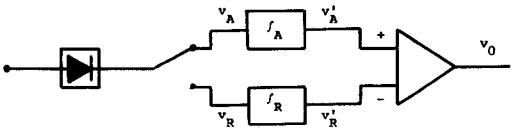

Fig. 9. Post detection voltages.

$$\phi_{v_{AR}}(\tau) = \langle (q_A(t)+q_n(t))^2 (q_R(t+\tau)+q_n(t+\tau))^2\rangle$$
$$\cdot\langle 1+g(t)g(t+\tau)\rangle$$
$$\cdot\langle d(1-d) - \tilde{p}(t)\tilde{p}(t+\tau)\rangle$$
$$= \left(2\phi_n^2(\tau) + (\mu_A+\mu_n)(\mu_R+\mu_n)\right)$$
$$\cdot(1+\phi_g)\cdot\left(d(1-d)-\phi_{\tilde{p}}\right). \tag{A15}$$

The output voltage v_0 is given by

$$v_0 = v'_A - v'_R \qquad \text{(see Fig. 9)}. \tag{A16}$$

The power spectrum S_{v0} of v_0 is given by the spectra of v'_A and v'_R according to

$$S_{v0}(f) = S_{vA'}(f) + S_{vR'}(f) - \left(S_{vA'R'}(f) + S^*_{vA'R'}(f)\right). \tag{A17}$$

The transformation function of the integrators include the weighting factors $1/d$ and $1/1-d$ and are described by

$$L_A(f) = \frac{1}{d}\frac{1}{\tau_A}\int_0^{\tau_A} e^{-j\omega t}\,dt = \frac{1}{d}e^{-j\pi f\tau_A}\operatorname{sinc}(\pi f\tau_A) \tag{A18}$$

$$L_R(f) = \frac{1}{1-d}\frac{1}{R}\int_0^{\tau_R} e^{-j\omega t}\,dt = \frac{1}{1-d}e^{-j\pi f\tau_R}\operatorname{sinc}(\pi f\tau_R). \tag{A19}$$

The power spectrum of S_{v0} can thus be expressed by the power spectra of v_A and v_R by

$$S_{v0}(f) = |L_A(f)|^2\frac{1}{d^2}S_{vA}(f) + |L_R(f)|^2\frac{1}{(1-d)^2}S_{vR}(f)$$
$$-\left(L_A(f)\cdot L_R^*(f)\cdot S_{vAR}(f)\right.$$
$$\left.+ L_A^*(f)\cdot L_R(f)\cdot S^*_{vAR}(f)\right)\frac{1}{d(1-d)}. \tag{A20}$$

By inserting (2) and (3) in (A11), S_{vA} can be calculated according to (A21)

$$S_{vA}(f) = \left((\mu_A+\mu_\eta)^2\delta(f) + 2\left(\frac{1}{2}k(T_A+T_n)\right)^2 G^*G\right)$$
$$\times *\left(\delta(f)+s_g(t)\right)^*$$
$$\cdot\left(\delta(f) + \sum_{n\neq 0}\operatorname{sinc}^2(n\pi d)\delta(f-nf_m)\right)d^2 \tag{A21}$$

where * denotes the folding operation

$$a^*b(\tau) = \int_{-\infty}^{\infty} a(t)b(\tau - t)\,dt. \tag{A22}$$

By inserting (A21) and the equivalent expressions for S_{v_R}

and $S_{v_{AR}}$ into (A20) we arrive at

$$
\begin{aligned}
S_{v0}(f) = &\left(\frac{1}{2}k(T_A - T_R)\int G(f)\,df\right)^2 \cdot \delta(f) \\
&+\left(\frac{1}{2}k\int G(f)\,df\right)^2 \\
&\cdot\Big[(T_A+T_n)^2\cdot \operatorname{sinc}^2 \pi f\tau_A + (T_R+T_n)^2\cdot \operatorname{sinc}^2 \pi f\tau_R \\
&-2(T_A+T_n)(T_R+T_n)\cos(\pi f(\tau_R-\tau_A)) \\
&\cdot \operatorname{sinc}\pi f\tau_A \cdot \operatorname{sinc}\pi f\tau_R\Big]\cdot S_g(f) \\
&+\Big[\frac{1}{2}k^2\Big\{(T_A+T_n)^2\operatorname{sinc}^2(\pi f\tau_A) \\
&+(T_R+T_n)^2\operatorname{sinc}^2(\pi f\tau_R) \\
&-2\cdot\cos(\pi f(\tau_A-\tau_R))\cdot\operatorname{sinc}(\pi f\tau_A) \\
&\cdot\operatorname{sinc}(\pi f\tau_A)\cdot T_n^2\Big\} G^*G \\
&+\left(\frac{1}{2}k\int G df\right)^2\Big\{\left(\frac{T_A+T_n}{d}\right)^2\sin^2(\pi f\tau_A) \\
&+\left(\frac{T_R+T_n}{1-d}\right)^2\cdot\operatorname{sinc}^2(\pi f\tau_R) \\
&+2\cos(\pi f(\tau_A-\tau_R))\cdot\operatorname{sinc}(\pi f\tau_A) \\
&\cdot\operatorname{sinc}(\pi f\tau_R)\frac{(T_A+T_n)(T_R+T_n)}{d(1-d)}\Big\}S_{\tilde{p}} \\
&+\frac{1}{2}k^2\Big\{\left(\frac{T_A+T_n}{d}\right)^2\operatorname{sinc}^2(\pi f\tau_A) \\
&+\left(\frac{T_R+T_n}{1-d}\right)^2\cdot\operatorname{sinc}^2(\pi f\tau_R) \\
&+2\cos(\pi f(\tau_A-\tau_R))\operatorname{sinc}(\pi f\tau_A) \\
&\cdot\operatorname{sinc}(\pi f\tau_R)\frac{T_n^2}{d(1-d)}G^*G^*S_{\tilde{p}}\Big] \\
&*(\delta(f)+S_g(f)). \qquad \text{(A23)}
\end{aligned}
$$

The first term of (A23) describes the mean value of v_0 according to (A10) while the remainder term describes the deviation of the output signal. By integrating (A23) with respect to frequency, (A24) is obtained.

Noting that $(\Delta G/G)^2 \ll 1$ and $\Sigma_{n\neq 0} d^2\operatorname{sinc}^2(n\pi d) = d(1-d)$, (A24) may be simplified to

$$
\begin{aligned}
\sigma_{v0}^2 = &\frac{1}{2}k^2\int G^2\,df\left[\frac{(T_A+T_n)^2}{d\cdot\tau_A}+\frac{(T_R+T_n)^2}{(1-d)\cdot\tau_R}\right] \\
&+\left(\frac{1}{2}k\int G\,df\right)^2\cdot 2\Big[(T_A+T_n)^2\int_{1/2\tau_R}^{1/2\tau_A} S_g(f)\,df \\
&+(T_A-T_R)^2\int_0^{1/2\tau_R} S_g(f)\,df\Big] \\
&\times\left(\frac{1}{2}k\int G\,df\right)^2\cdot\Big[\Sigma d^2\sin^2 c(n\pi d) \\
&\cdot\Big[\left(\frac{T_A+T_n}{d}+\frac{T_R+T_n}{1-d}\right)^2\frac{1}{\tau_R} \\
&+\left(\frac{T_A+T_n}{d}\right)^2\left(\frac{1}{\tau_A}-\frac{1}{\tau_R}\right)\Big]\cdot\bar{S}_g(nf_m)\Big]. \qquad \text{(A25)}
\end{aligned}
$$

By inserting (A10) and (A25) into (6), the resolution of the radiometer is found according to (7).

References

[1] Coastal Oceans Monitoring Satellite System (COMSS), Phase A Study, British Aerospace Dynamics Group, ESA Contract No. 3632/78/F/EG, Document Ref. ESS/SS 930, Mar. 1979.

[2] J. H. Reinwater, "Radiometers: Electronic eyes that see noise," *Microwave*, p. 59, Sept. 1978.

[3] Staelin *et al.*, "High resolution passive microwave satellite," Massachusetts Institute of Technology, Report for NASA, Contract NAS 5-23677, Apr. 1978.

[4] J. M. Schuchardt and J. A. Stratigos, "Detected noise levels guide radiometer design," *Microwave*, p. 64, Sept. 1978.

[5] G. Evans and C. W. McLeish, *RF-Radiometer Handbook.* New York: Artech House, 1977.

[6] J. W. Sherman, "Passive microwave sensors for satellites," in *Proc. Sixth Int. Symp. on Remote Sensing of Environment*, vol. 2, pp. 651–659.

[7] S. Axelsson and O. Edvardsson, "Passive microwave radiometry and its potential applications to earth resources surveys," Basic Physics and Technology, ESTEC Contract No. 1411/71.

[8] A. Magun and K. Kuenzi, "Influence of statistical gain fluctuations of the high-frequency amplifier on the sensitivity Dicke-radiometer," *Z. Ange. Math. Phys.*, vol. 22, pp. 392–403, 1971.

[9] G. M. Hidy, W. F. Hall, W. N. Hardy, W. W. Ho, A. C. Jones, A. W. Love, M. J. Van Melle, H. H. Wang, and A. E. Wheeler, "Development of a satellite microwave radiometer to sense the surface temperature of the world oceans," NASA Contractor Report NASA CR-1960.

[10] Nelson M. Blachman, *Noise and Its Effect on Communication.* New York: McGraw-Hill, 1966.

[11] M. E. Tiuri, "Radiometer astronomy receivers," *IEEE Trans. Antennas Propagat.*, vol. AP-12, p. 930, 1964.

[12] M. H. Graham, "Radiometer circuits," *Proc. IRE*, vol. 46, p. 1966, 1958.

[13] M. J. Yerbury, "A gain-stabilising detector for use in radio astronomy," *Rev. Sci. Instr.*, vol. 46, no. 2, Feb. 1975.

[14] N. Skou, "Development of an airborne multifrequency radiometer system," Electromagnetics Institute, Technical University of Denmark, Dec. 1978.

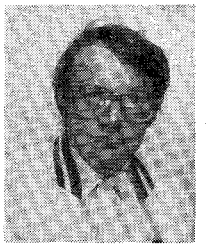

Flemming Thomsen (M'82) was born in Copenhagen, Denmark, on December 25, 1950. He received the Master of Science degree from the Technical University of Denmark in 1975.

From 1977 to 1980, he was a Research Associate at the Technical University of Denmark, Electromagnetics Institute. He is presently employed by the Royal Danish Airforce and working with radar systems.